J. Chem. Sci. Vol. 127, No. 4, April 2015, pp. 751–759.
DOI 10.1007/s12039-015-0831-0

Hydrogen adsorption of nitrogen-doped carbon nanotubes functionalized with 3d-block transition metals

MICHAEL R MANANGHAYA
De La Salle University-Manila, Taft Ave., Manila 1004, Philippines
e-mail: mikemananghaya@gmail.com

MS received 14 May 2014; revised 9 October 2014; accepted 24 November 2014

Abstract. A systematic study of the most stable configurations, calculation of the corresponding binding and free energies of functionalized 3d transition metals (TMs) on (10,0) Single Walled Carbon Nanotube (SWCNT) doped with porphyrin-like nitrogen defects (4ND-CN_xNT) using spin-polarized density functional theory (DFT) formalism with flavours of LDA and GGA exchange-correlation (XC) functionals has been made. A thorough analysis showed that the electronic and magnetic properties of SWCNT are dependent on the TMs absorbed wherein, the composite material TM/4ND-CN_xNT can act as a medium for storing hydrogen at room temperature manifested through favourable adsorption energy.

Keywords. Binding energy; density functional theory; porphyrin defects; transition metals

1. Introduction

Introduction of defects and dopants can alter the electronic and magnetic properties of Single walled Carbon Nanotubes (SWCNT). Recently, efficient ways to modify the properties of carbon nanotubes (CNT) have attracted various groups of considerable interest.[1–6] B and/or N have roughly the same atomic radius as C atoms. Specifically, N is a good choice of dopant that is expected to make semiconducting CNT metallic due to its one extra electron compared to a C atom.[1–5] The N-doped CNT (CN_xNT) has been synthesized in several groups[7–12] using various approaches including magnetron sputtering,[13] pyrolysis of nitrogen-rich organic chemicals,[14] and arc-discharge in nitrogen atmosphere.[15] However, most of the syntheses yield nitrogen-doped multi-walled carbon nanotubes ($MWCN_x$NT) with bamboo-shaped morphology. Recently, the synthesis of nitrogen-doped SWCNT bundles via an aerosol-assisted chemical vapour deposition (CVD) method was reported.[16] It has been suggested that the nitrogen dopants are substituted into the carbon network with and without vacancy formation identified by electron energy loss spectroscopy and X-ray photoelectron spectroscopy measurements.[9,10] Vacancy structures co-exist both as pyridine-like and porphyrin-like wherein the porphyrin-like nitrogen substitution accompanied with vacancy (4ND) formed in the sidewall of SWCNT is a four-nitrogen divacancy. The electronic,[17] field emission[18] and electrical transport properties[19] of these structures have been investigated systemically. The presence of 4ND defects in CNT, suggests that the reactivity might be greatly enhanced compared to the pure CNT.[16,20–28] The introduction of new levels close to the Fermi level with nitrogen doping can change the sensibility of CNT to different kinds of molecules.[16,20,21] Modification of the electronic and magnetic properties of CNT can also typically be effectively modified through chemical decoration of transition metals (TMs),[29–31] which greatly expands the potential application areas of CNT, such as improving the sensitivities of chemical sensors, developing spintronic devices or catalysts and providing higher reactive sites for hydrogen gas storages.[24–28,32–37] 4ND defects in nitrogen-doped nanostructures may enhance reactivity and immobilize species such as transition metals;[29–31] also the binding strengths of TMs with SWCNT doped with porphyrin-like nitrogen defects (4ND-CN_xNT) are significantly enhanced when compared to the pure SWCNT such that binding is stable and favourable dictated by a strong binding energy that could improve transition metal dispersion over the metal decorated SWCNT. Theoretical calculations revealed that the 4ND defects in SWCNT resulted in a decreased value of band gaps and the electronic properties of SWCNT can be effectively modified, which are strongly dependent on the TMs absorbed.[38–43]

The incorporation of nitrogen and transition metal atoms into carbon nanotubes affords structures with the ability to participate in hydrogen bonding. TM-dispersed materials have been studied recently for large

hydrogen storing capacity with respect to the release temperature, the TM-H_2 binding energy and ratio which look very promising.[32–37] US Department of Energy (DOE) Hydrogen Plan has set a standard for this discussion by providing a commercially significant benchmark for the amount of reversible hydrogen adsorption. The benchmark for the ratio of stored hydrogen weight to system weight requires an efficiency of 6.5 wt% hydrogen and a volumetric density of 62 kg H_2/m^3. A systematic study of the most stable configurations, calculation of the corresponding binding and free energies of functionalized 3d TMs on (10,0) 4ND-CN_xNT using DFT formalism is presented in the paper to show that the composite material TM/4ND-CN_XNT can act as a medium for storing hydrogen at room temperature.

2. Computational

Calculations were performed on supercells of zigzag (10,0) CNT with 4ND that is chemically functionalized with 10 different TMs (figure 1) using first-principles density functional theory (DFT), Dmol^3 code, available from Accelrys.[44] Experimentally produced CNTs have an average diameter of around 1 nm. Theoretically, calculated diameter close to 1 nm can be considered; obviously dictated by the need to drastically reduce the computational effort in such a large unit cell, single-walled (10,0) zigzag nanotube was chosen motivated by the small periodicity of the zigzag nanotubes compared to chiral ones. Thus the system is correspondingly small, which should justify the choice, as seen later on the discussion of the results. Each electronic wave function is expanded in a localized atom-centred basis set with each basis function defined numerically on a dense radial grid. For supercell geometries, spin-unrestricted calculations were carried out with a double numeric polarized (DNP) basis set available and the atomic cut-off set at 4.6 Å, along with gradient-corrected Perdew-Burke-Ernzerhof (PBE/GGA) functional.[45] Scalar relativistic effects were included via a local pseudopotential for all-electron calculations. Also, Perdew-Wang (PWC/LDA) parametization[46] was employed for exchange correlation with the same technicalities used in the calculation of (10,0) nanotube. The local-density approximation (LDA) functional depends only on the density at the coordinate where the functional is evaluated wherein the formulae arises from quantum Monte Carlo simulations. Generalized gradient approximations (GGA) on the other hand is still local but it takes into account the gradient of the density at the same coordinate which offers very good results for molecular geometries and ground-state energies. Both GGA and LDA are adapted to estimate the range of the adsorption energy, LDA gives slightly stronger interaction between H_2 and TM-doped nanotubes than GGA; conversely, the GGA underestimates the binding energy of H_2. The LDA and GGA flavours aide in interpreting if the final binding energies fall within the permissible adsorption energy at room temperature. A triclinic supercell of $30 \times 30 \times 12.78$ Å^3 was used to simulate the nanotube with infinite length, with a wall-to-wall distance of at least 10 Å, sufficient to avoid in-plane interactions between nanotubes in adjacent unit cells. The lattice parameter c equalled to fivefold of the periodicity of (10,0) SWCNT and the lattice parameters a and b were large enough to ignore the effect of neighbouring tubes. The Monkhorst-Pack scheme[47] was used in the Brillouin zone with $1 \times 1 \times 5$ special k-points for all geometry optimizations with the Broyden-Fletcher-Goldfarb-Shanno (BFGS) algorithm with convergence criterion of 0.005 Å on displacement, and 10^{-5} a.u. on the total energy and electron density. The Fermi levels of the spin-unrestricted band structures of (10,0) nanotubes were reset at the 0 eV position. The 4ND-CN_xNT was constructed as shown in figure 1a by deleting 2 carbon atoms and replacing the surrounding 4 C with 4 N. TM was then attached to each of the 4 N atoms of the 4ND-CN_xNT as presented in figure 1b.

3. Results and Discussion

Figure 1(a) shows the nitrogen-containing (10, 0) carbon nanotubes formed by $C_{114}N_4$ units 7.83 Å in diameter and 12.78 Å in length. The interlayer bond lengths calculated by density-functional theory for, C—C and C–N bonds are ∼1.425–1.429 Å and ∼1.338–1.352 Å, respectively. A typical (sp^3)C—C(sp^3) bond length is 1.54 Å. The C—N bond length for amines is 1.479 Å. Due to the two missing C atom, the C–N bond lengths of porphyrin-like doping are smaller. To analyze the bond lengths and bond angles, all nanotube geometries were optimized at the same level of theory, including porphyrin as a reference. Formation energies of the nitrogen-containing carbon nanotubes with pyridine-like and porphyrin-like vacancy were calculated for a (10,0) nitrogen-doped CNT. The formation energy of porphyrin-like vacancy is 3.10 eV while the pyridine-like vacancy is around 3.17 eV. The formation-energy values have a close relationship to the nanotube structures in this study. These indicate that formation of a divacancy is preferred over monovacancy and the dangling bonded carbon atoms near the divacancies would be replaced with four nitrogens from N_2 molecules in

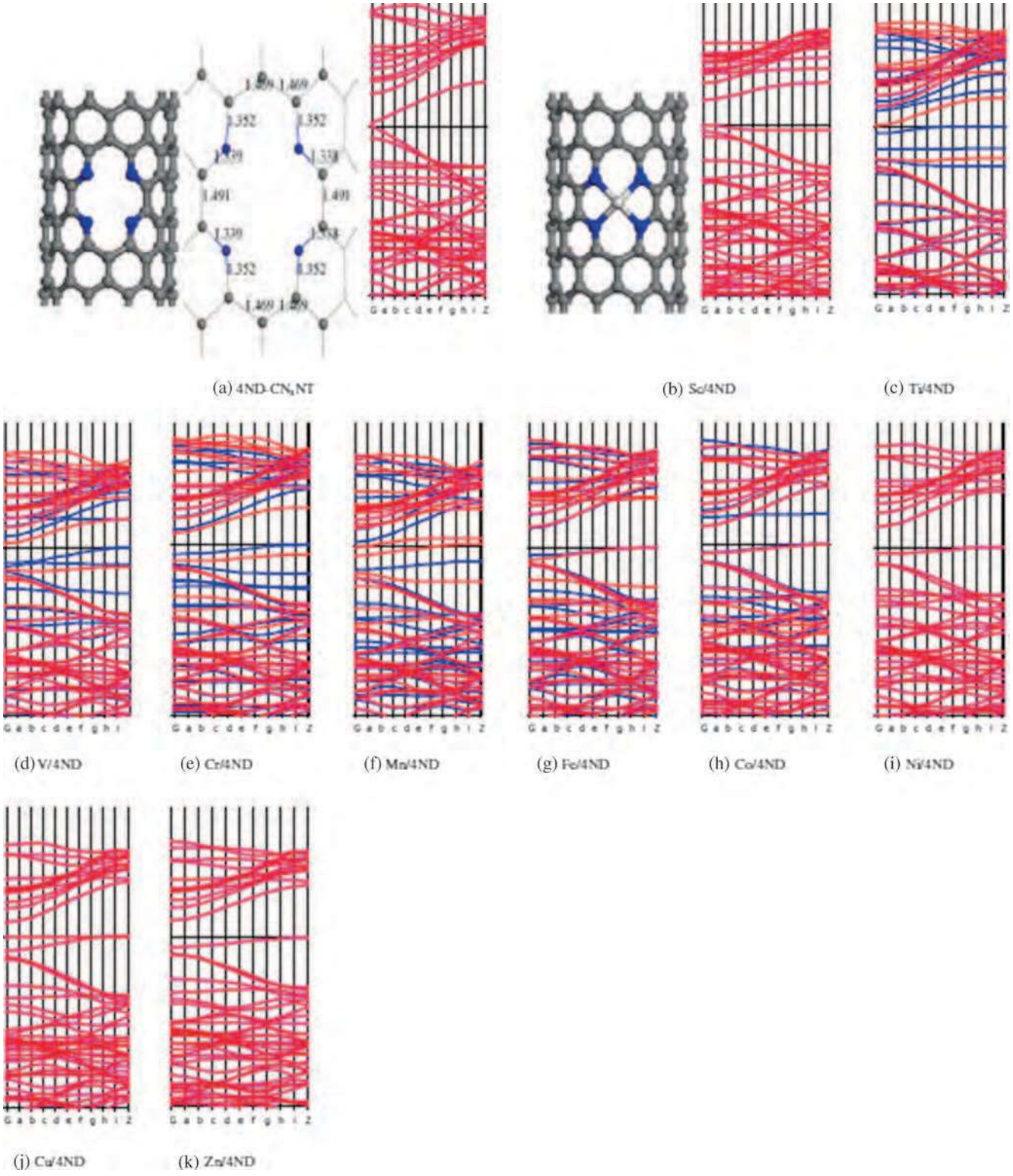

Figure 1. (a) Geometrically optimized structure and bond lengths (Å) of N substitution into the carbon framework with the formation of porphyrin-like vacancy. A fragment of the supercell was taken out to elucidate the bond lengths at the vicinity of the N/TM impurities and (b) to (k) band structures of 10 TMs adsorbed on (10, 0) zigzag CN_xNT with porphyrin-like defect. The Fermi level is set as zero and plotted with a broken line. The blue and red plots denote alpha and beta band structures, respectively. Only one part indicates that this system is non-magnetic. Energies at the vertical axis are at arbitrary units.

the gas phase in the presence of catalysts or iron oxides. Hirshfeld population analysis shows that charge is of the order 0.116 e on each of the four nitrogen atoms of 4ND-CN_xNT. Hence, this site of the nanotube is very reactive as it can act as a strong oxidizing agent for transition metal atoms.

As TM atom is adsorbed on the CN_xNT, two kinds of initial configurations were considered: (1) the TM is directly bound to the site of 4ND; (2) the TM is attached to the sites near 4ND. After full structural optimization, the TM adsorptions on the defect sites are the most stable because of their higher reactivity than other sites.[16,20,21,38–43] Based on the comparison of the bond angles and bond lengths of porphyrin, the structure with porphyrin-like defect functionalized with TM can be observed as shown in figure 1b for Sc has an increase in the C–N bond lengths of nanotube which is ∼1.384–1.400 Å although it has a smaller bond lengths than amine. Impurities in CNTs produce their own local strains as expected for these structures as shown in table 1; the structural parameters of most stable configurations of TMs adsorbed on 4ND-CN_xNT (labelled as TM/4ND-CN_xNT) is characterized by forming multiple TM–N bonds at the hollow sites wherein all the TMs are projecting from the sidewall of the 4ND-CN_xNT in various ways. The average TM–N distances (D_{TM-N}) of TM/4ND-CN_xNT range from GGA-1.923 (Ni) to 2.144 (Sc) Å and LDA-1.918 (Ni) to 2.120 (Sc) Å. Thus it can be surmised that N and TM impurities in CNT produce respective deformations. The binding energy (E_b) of an individual TM on the 4ND-CN_xNT is defined as:

$$E_b = E(4ND - CN_xNT) + E(TM) - E(TM/4ND - CN_xNT), \quad (1)$$

where E denotes the total energy of the optimized system the bracket. In table 1, $E_b > 0$ for all indicates a stable optimized configuration and bonding. On the other hand, due to the N participation and the vacancy defect, the binding energies of all TMs on the 4ND-CN_xNTs are generally larger than those on the pure CNT[48–53] such that the presence of porphyrin-like nitrogen defects is crucial for enhancing the metal binding to the defects. The CN_xNT with 4ND defects uses two valence electrons to form a lone pair wherein strong interaction exists between p orbitals of N atoms and the d orbitals of various TMs due to their hybridization with each other.

Table 1. Average TM–N distances (D_{TM-N}) of TM/4ND-CN_xNT, binding energy (E_b) of an individual TM on the 4ND-CN_xNT, calculated charge transfer using Hirshfeld population analysis, the charges transferred from TMs to the (10,0) CN_xNT with 4ND defect (C_{TM}), and total magnetic moment ($\mu_{total\ \mathbf{TM}}$). Average distance between the TM and H_2($\boldsymbol{D}_{\mathbf{TM-H2}}$), average adsorption energies per H_2 on TM-decorated CN_x nanotube with porphyrine-like defects, charge transferred from TMs to the (10,0) CN_xNT in the presence of H_2 ($\mathbf{C}_{\mathbf{TM-H2}}$), total magnetic moment ($\mu_{total\ TM-H2}$) in the presence of H_2, H-H distances ($\boldsymbol{D}_{\mathbf{H2}}$), and charge transferred from from H_2 to TM atom ($\mathbf{C}_{H2}$) using GGA (top) and LDA (bottom).

TM	$\boldsymbol{D}_{\mathbf{TM-N}}$ (Å)	$\mathbf{E}_{\mathbf{b-TM}}$ (eV)	$\mathbf{C}_{\mathbf{TM}}$ (e)	$\mu_{total\ \mathbf{TM}}$	$\boldsymbol{D}_{\mathbf{TM-H2}}$ (Å)	$\mathbf{E}_{\mathbf{b-H2}}$ (eV)	$\mathbf{G}_{\mathbf{b-H2}}$ (eV)	$\mathbf{C}_{\mathbf{TM-H2}}$ (e)	$\mu_{total\ TM-H2}$	$\boldsymbol{D}_{\mathbf{H2}}$ (Å)	$\mathbf{C}_{H2}$ (e)
Sc	2.144	8.765	0.704	0	2.324	0.239	0.302	0.573	0	0.766	0.059
Ti	2.075	8.256	0.517	1.516	1.921	0.536	0.649	0.418	0	0.828	0.022
V	2.059	7.801	0.381	2.470	1.954	0.228	0.269	0.290	2.364	0.786	0.047
Cr	2.054	5.945	0.470	0.948	1.866	0.238	0.355	0.430	0	0.808	0.012
Mn	1.991	6.353	0.294	2.915	2.179	0.105	0.128	0.243	0	0.764	0.034
Fe	1.967	7.397	0.231	1.911	1.630	0.311	0.376	0.142	0	0.837	0.044
Co	1.950	7.598	0.195	0.9694	1.885	0.198	0.244	0.150	0.917	0.778	0.037
Ni	1.923	7.089	0.127	0	3.143	0.013	0.091	0.131	0	0.750	0.004
Cu	2.030	4.607	0.360	0	2.075	0.067	0.346	0.346	0	0.764	0.046
Zn	2.056	3.495	0.472	0	2.212	0.119	0.118	0.442	0	0.759	0.037
Sc	2.120	10.437	0.680	0	2.199	0.408	0.425	0.515	0	0.788	0.060
Ti	2.044	10.052	0.496	1.545	1.761	0.869	1.016	0.380	0	0.865	0.018
V	2.046	8.515	0.341	2.755	1.725	0.809	0.846	0.278	0.018	0.890	0.010
Cr	2.019	7.876	0.433	0.964	1.704	0.970	1.326	0.405	0.047	0.866	0.013
Mn	1.968	8.387	0.254	2.983	1.958	0.589	0.723	0.114	0.004	0.873	0.022
Fe	1.941	9.463	0.196	1.954	1.584	1.058	1.212	0.116	0	0.872	0.042
Co	1.924	9.732	0.165	0.977	1.736	0.583	0.590	0.113	0.870	0.815	0.036
Ni	1.918	8.607	0.104	0	2.903	0.517	0.857	0.103	0	0.768	0.002
Cu	1.991	5.712	0.349	0.002	1.849	0.255	0.436	0.322	0	0.795	0.015
Zn	2.025	4.333	0.443	0	2.012	0.333	0.430	0.403	0	0.781	0.018

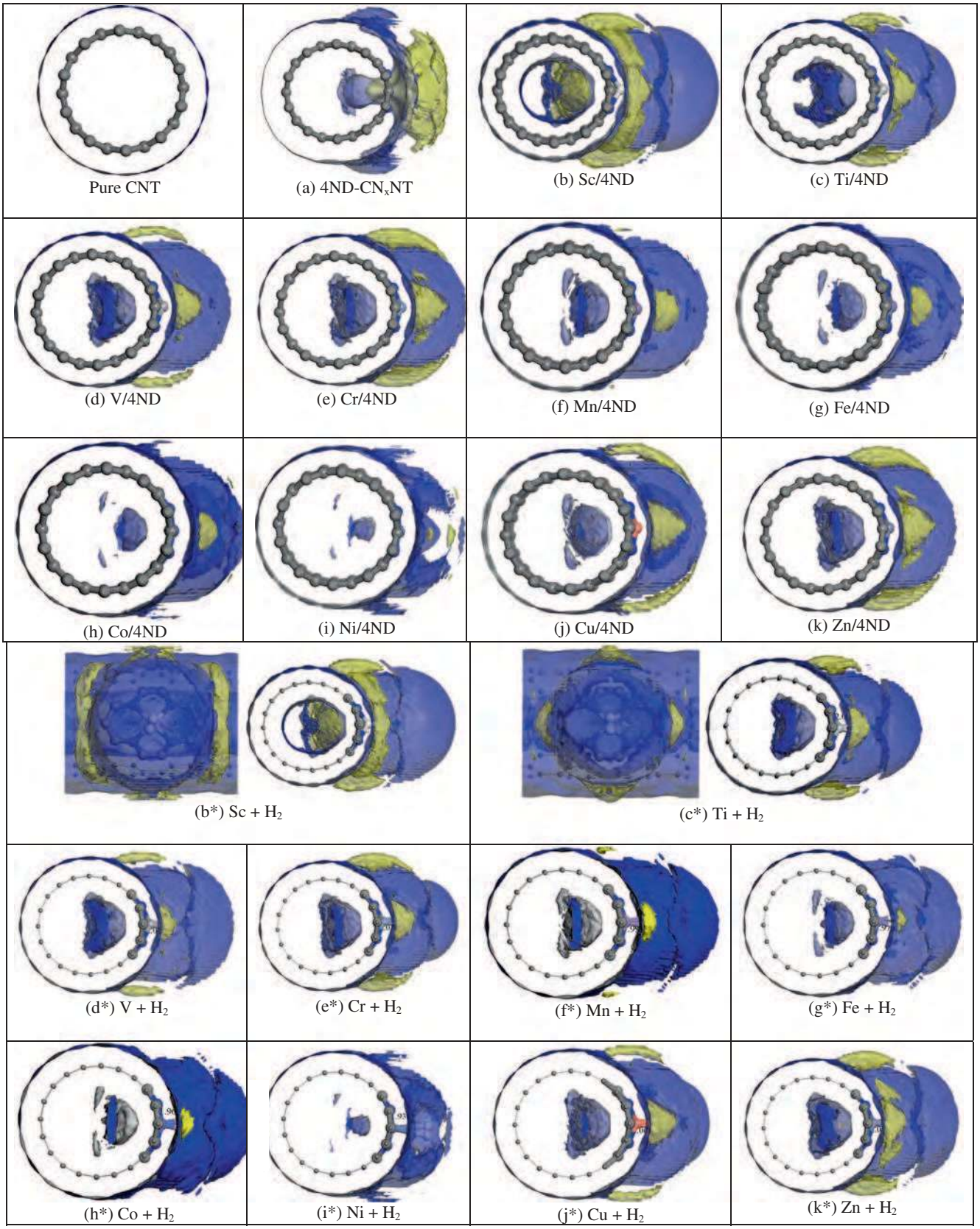

Figure 2. Surface electrostatic potentials of the nitrogen-doped carbon nanotubes functionalized with 3d-block transition metals with and without adsorption of hydrogen using the generalized gradient approximations.

In figures 1b–1k: the band structures of different TM/CN_xNT nanotubes are represented. It can be seen that upon adsorption of these TMs on CN_xNT, the electronic properties are changed to different degrees that is strongly dependent on the adsorbed TMs, certain impurity states are introduced into their band structures, rendering the electronic properties to change to different degrees that are strongly dependent on the adsorbed TMs. For example, when Sc, Ni, Cu, Zn are adsorbed on the two CN_xNTs, several semiconductors nanocomposites are obtained as their band gaps are increased to different degrees due to the lift of the conduction bands of CN_xNTs. Interestingly, for Mn adsorptions the influences on electronic properties is completely different: has a half-metallic character. This means that CN_xNT-based devices with various electronic properties can be achieved. The changes in band structures of the CN_xNT upon adsorption of these TMs are also evident by the charge transfer between the TM and the CN_xNT. As shown in table 1, in which we list the calculated charge transfer using Hirshfeld population analysis,[54] the charges transferred from TMs to the (10,0) CN_xNT with 4ND defect range from GGA-0.127 e (Ni) to 0.704 e (Sc) and LDA-0.104 e (Ni) to 0.680 e (Sc) which are evident from the surface electrostatic potentials (SEP) shown in figures 2–3. The delocalized SEP of pure (10,0) nanotube is changed to a polarized form as 4ND defects were introduced shortly after the Sc functionalization, the polarization of the SEP is more enhanced towards the 4ND-Sc dopant indicating partially cationic character of the TMs due to the charge transfer, which facilitates the adsorption of foreign species such as hydrogen gas as discussed next. It is worth noticing that the polarization is weakest at Ni dopant which has a low charge transfer as mentioned before and as observed in both GGA and LDA plots in figure 2–3. When one H_2 molecule is adsorbed on the TM/4ND-CN_xNT system, the H-H bond length is elongated from 0.752 Å of a free H_2 to as high as GGA-0.828 Å (Ti) and LDA-0.890 Å (V) as displayed in table 1. Optimized TM-H_2 bond length is found to range from GGA-1.630 (Fe) to 3.143 (Ni) Å and LDA-1.584 (Fe) to 2.903 (Ni) Å. It is seen in the table depending on the TM incorporated that GGA-0.004e (Ni) to 0.059e (Sc) and LDA-0.002e (Ni) to 0.060e (Sc) charge are transferred from H_2 to TM atom and the entire TM atoms still carry a positive charge ($\mathbf{C_{TM-H2}}$), indicating that more H_2 molecules can be absorbed as can be visualized in the SEP. Interestingly, Sc posses the maximum electron transferred of about GGA-0.573 e and LDA-0.515 e, the average adsorption energies per H_2 based on PBE-GGA calculations ranges from 0.013 to 0.536 eV and adsorption energies per H_2 based on LDA-PWC ranging from 0.255 to 1.058 eV was obtained and summarized in table 1. The maximum number of H_2 molecules that can be bound to the TM/4ND-CN_xNT system was calculated using Sc as the representative to show how much N-doped units can be introduced per unit quantity and how much H_2 adsorption can it facilitate. The number of H_2 was gradually increased to address the maximum number of H_2 molecules that can bound to the Sc/4ND-CN_xNT system and after full relaxation for every H_2 adsorption configuration, the GGA predicted that the Sc atom could absorb up to five H_2. Correspondingly, based on GGA-PBE calculations the average adsorption energies per H_2 ranges from 0.097 ($5H_2$-Sc/4ND-CN_xNT) to 0.239 ($1H_2$-Sc/4ND-CN_xNT) eV in good agreement within the adsorption requirement of hydrogen storage at room temperature of 0.20 $\sim$0.70 eV/H_2.[55] Most importantly, the H-H distances are increased slightly from 0.752 Å to 0.758 Å due to the charge transfer from the H_2 molecules to the Sc/4ND-CN_xNT yet all the adsorbed H_2 remain molecular. The adsorption of H_2 molecules was studied further on a 5 Sc functionalized to a CN_xNT with 5 4ND defects. In this case, each Sc atom carries a positive charge of 0.658 e. Five H_2 was placed on each Sc atom. A starting configuration for geometry optimization is taken by attaching H_2 as high as 25 around the Sc atoms above the five defects, the hydrogen atoms remain molecular with an average bond length of around 0.755 Å with average hydrogen adsorption energy of 0.092 eV per H_2 calculated using GGA-PBE functional the resulting calculation is also verified using LDA as support and it is still in good agreement with the adsorption requirement of hydrogen storage.[55]

On the other hand, free energy values for binding was obtained to serve as a guide to experimentalists are shown in table 1. The free energy ranges from GGA-0.091 to 0.649 eV and LDA-0.425 to 1.326 eV. Also, the effects of TM adsorption on the magnetic properties of CN_xNT is evaluated and found that the net magnetic moment emerges, ranging from GGA-2.915, LDA-2.983 (for Mn/4ND-CN_xNT) to 0 μB (for Sc/, Ni/, Cu/ and Zn/4ND-CN_xNT) for the net magnetic moment in the presence of H_2, ranges from GGA-2.364 (for V/4ND-CN_xNT), LDA-0.870 (for Co/4ND-CN_xNT) to 0 μB for the other TMs. This is reasonable, because the ground states of the CN_xNTs are non-magnetic, and the net spin magnetic moment mainly originates from the contributions of TMs. The net magnetic moment decreases as the system takes up a H_2 wherein a drastic change is experienced in the Fe case for example where the value drops to zero.

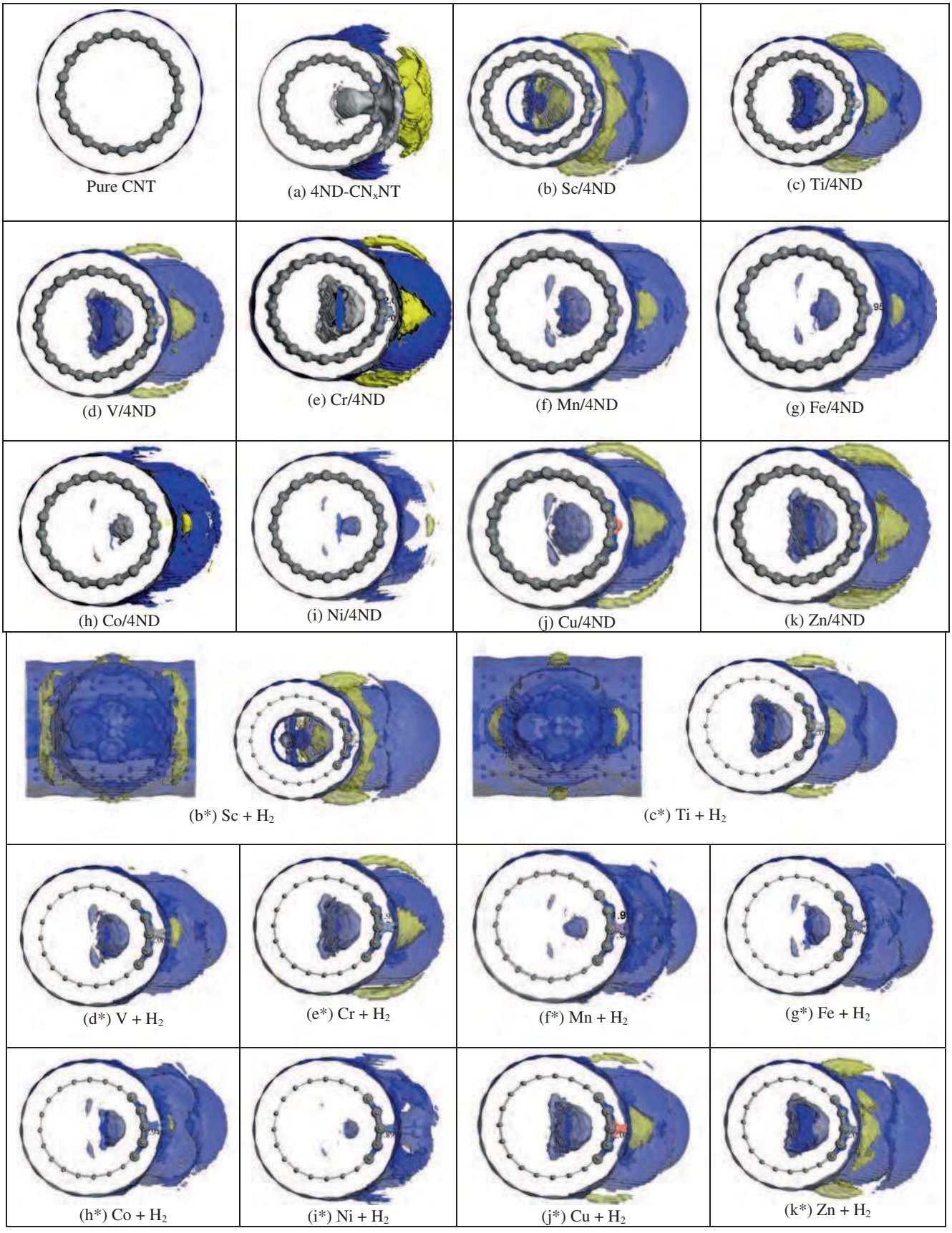

Figure 3. Surface electrostatic potentials of the nitrogen-doped carbon nanotubes functionalized with 3d-block transition metals with and without adsorption of hydrogen using the local-density approximation.

4. Conclusions

The structural, electronic and magnetic properties of the (10,0) nanotube with porphyrin-like nitrogen defects functionalized with 3d block TMs (Sc, Ti, V, Cr, Mn, Fe, Co, Ni, Cu, and Zn) are systemically studied, using density functional theory. Porphyrin defects in SWCNT caused an enhanced transition metal binding and the chemical functionalization of all TMs is thermodynamically stable. The electronic and magnetic properties of TMs on 4ND-CN_xNT can be effectively modified which shows interesting possibilities of tailoring the properties of CNT by TM doping. Binding of hydrogen molecules to the composite material TM/4ND-CN_XNT was observed within the adsorption requirement of hydrogen storage at room temperature suggesting a potential storage media for hydrogen.

References

1. Tasis D, Tagmatarchis N, Bianco A and Prato M 2006 *Chem. Rev.* **106** 1105
2. Zhao Y L and Stoddart J F 2009 *Acc. Chem. Res.* **42** 1161
3. Khabashesku V N, Billups W E and Margrave J L 2002 *Acc. Chem. Res.* **35** 1087
4. Niyogi S, Hamon M A, Hu H, Zhao B, Bhowmik P, Sen R, Itkis M E and Haddon R C 2002 *Acc. Chem. Res.* **35** 1105
5. Dong L, Craig M M, Khang D and Chen C J 2012 *Nanotechnology* **2012** 1
6. Mananghaya M, Rodulfo E, Santos G N and Villagracia A R 2012 *J. Nanotechnol.* **2012** 780815
7. Sen R, Satishkumar B C, Govindaraj A, Harikumar K R, Renganathan M K and Rao C N R 1997 *J. Mater. Chem.* **12** 2335
8. Terrones M, Terrones H, Grobert N, Hsu W K, Zhu Y Q, Hare J P, Kroto H W, Walton D R, Ph Kohler-Redlich M W, Rühle M, Zhang J P and Cheetham A K 1999 *Appl. Phys. Lett.* **75** 3932
9. Czerw R, Terrones M, Charlier J C, Blasé X B, Foley R, Kamalakaran N, Grober H, Terrone D, Tekleab P M, Ajayan W, Blau M and Carrroll D L 2001 *Nano. Lett.* **1** 457
10. Terrones M, Ajayan P M, Banhart F, Blase X, Carroll D L, Charlier J C, Czerw R, Foley B, Grobert N, Kohler-Redlich Ph, Rühle M, Seeger T and Terrones H 2002 *Appl. Phys. A Mater. Sci. Process* **74** 355
11. Golberg D, Dorozhkin P S, Bando Y, Dong Z C, Tang C C, Uemura Y, Grobert N, Reyes M, Terrones H and Terrones M 2003 *Appl. Phys. A Mater. Sci. Process* **76** 499
12. Villalpando-Páez F, Romero A H, Mnŏz-Sandoval E, Martínez L M, Terrones H and Terrones M 2004 *Chem. Phys. Lett.* **386** 137
13. Suenage K, Johansson M P, Hellgren N, Broitman E, Wallenberg L R, Colliex C, Sundgren J and Hultman L 1999 *Chem. Phys. Lett.* **300** 695
14. Lim S H, Elim H I, Gao X Y, Wee A T S, Ji W, Lee J Y and Lin J 2006 *Phys. Rev. B* **73** 045402
15. Droppa Jr. R, Ribeiro C T M, Zanatta A R, dos Santos M C and Alvarez F 2004 *Phys. Rev. B* **69** 045405
16. Villalpando-Paez F, Zamudio A, Elias A L, Son H, Barros E, Chou B S G, Kim Y A, Muramatsu H, Hayashi T, Kong J, Terrones H, Dresselhaus G, Endo M, Terrones M and Dresselhaus M S 2006 *Chem. Phys. Lett.* **424** 345
17. Yu S S, Wen Q B, Zheng W T and Jiang Q *Nanotechnology* **18** 165702
18. Qiao L, Zheng W T, Xu H, Zhang L and Jiang Q 2007 *J. Chem. Phys.* **126** 64702
19. Min Y S, Bae E J, Kim U J, Lee E H, Park N J, Hwang C S and Park W J 2008 *Appl. Phys. Lett.* **93** 043113
20. Rocha A R, Rossi M, Fazzio A and da Silva A J R 2008 *Phys. Rev. Lett.* **100** 176803
21. Li Y F, Zhou Z and Wang L B 2008 *J. Chem. Phys.* **129** 104703
22. Gong K P, Du F, Xia Z X, Durstock M and Dai L M *Science* **323** 760
23. Ayala P, Arenal R, Rümmeli M, Rubio A and Pichler T 2010 *Carbon* **48** 575
24. Yoon H, Ko S and Jang J 2007 *Chem. Commun.* **14** 1468
25. Shao Y, Sui J, Yin G and Gao Y 2008 *Appl. Catal. B* **78** 89
26. Su F B, Tian Z Q, Poh C K, Wang Z, Lim S H, Liu Z L and Lin J Y 2010 *Chem. Mater.* **27** 832
27. Li X G, Park S and Popov B N 2010 *Power Source* **195** 445
28. Shao Y Y, Liu J, Wang Y and Lin Y H 2009 *J. Mater. Chem.* **19** 46
29. Gregory G, Wildgoose C, Banks E and Richard G C 2006 *Small* **2** 182
30. Georgakilas V, Gournis D, Tzizios V, Pasquato L, Guldi D M and Prato M 2007 *J. Mater. Chem.* **17** 2679
31. White R J, Luque R, Budairn V L, Clark J H and Macquarrie D J 2009 *Chem. Soc. Rev.* **38** 481
32. Yue B, Ma Y W, Tao H S, Yu L S, Jian G Q, Wang X Z, Wang X S, Lu Y N and Hu Z 2008 *J. Mater. Chem.* **18** 1747
33. Jiang J S, Ma Y W, Jian G Q, Tao H S, Wang X Z, Fan Y N, Lu Y N, Hu Z and Chen Y 2009 *Adv. Mater.* **21** 4953
34. Zhou Y, Pasquareli R, Holme T, Berry J, Ginley D and O'Hayre R 2009 *J. Mater. Chem.* **19** 7830
35. Lepró X, Terrés E, Vega-Cantú Y, Rodríguez-Macías F, Muramatsu H, Kim Y A, Hayahsi T, Endo M, Torres M and Terrones M 2008 *Chem. Phys. Lett.* **463** 124
36. Chen Z, Higgins D, Tao H S, Hsu R S and Chen Z W 2009 *J. Phys. Chem. C* **113** 21008
37. Sadek A Z, Zhang C, Hu Z, Partridge J G, McCulloch D G, Wlodarski W and Kalantar-zadeh K 2010 *J. Phys. Chem. C* **114** 238
38. Yang S H, Shin W H, Lee J W, Kim H S, Kang J K and Kim Y K 2007 *Appl. Phys. Lett.* **90** 013103
39. Li Y H, Hung T H and Chen C W 2009 *Carbon* **47** 850
40. Feng H, Ma J and Hu Z 2010 *J. Mater. Chem.* **20** 1702
41. Titov A V, Zapol P, Král P, Liu D J, Iddir H, Baishya K and Curtiss L A 2009 *J. Phys. Chem. C* **113** 21629
42. An W and Turner C H 2009 *J. Phys. Chem. C* **113** 7069
43. Stoyanov S, Titov A V and Kral P 2009 *Coord. Chem. Rev.* **253** 2852
44. Delley B 1990 *J. Chem. Phys.* **92** 508

45. Perdew J P, Burke K and Ernzerhof M 1996 *Phys. Rev. Lett.* **77** 3865
46. Perdew J P and Wang Y 1992 *Phys. Rev. B* **45**(23) 13244
47. Monkhorst H J and Pack J D 1976 *Phys. Rev. B* **13** 5188
48. Durgun E, Dag S, Bagci V, Gulseren T and Yildirim C S 2003 *Phys. Rev. B* **67** 201401
49. Durgun E, Dag S, Ciraci S and Gulseren O 2004 *J. Phys. Chem. B* **108** 575
50. Mananghaya M, Rodulfo E, Santos G N, Villagracia A R and Ladines A N 2012 *J. Nanomater.* **2012** 104891
51. Mananghaya M 2014 *Bull. Korean Chem. Soc.* **35**(1) 253
52. Mananghaya M 2012 *J. Korean Chem. Soc.* **56**(1) 34
53. Mananghaya M 2014 *J. Chem. Sci.* **126** 1737
54. Hirshfeld F L 1997 *Theor. Chim. Acta.* **44** 129
55. Zhao J, Ding Y, Wang X G, Cai Q and Wang X Z 2010 *Diamond Related. Mater.* **20** 3